Power System Protection and Control
ISSN:1674-3415

STUDY OF DRAG ON CONDUCTING FLUID FLOW PAST AN IMPERMEABLE CIRCULAR CYLINDER IN COMPOSITE REGIONS WITH MAGNETIC FIELD

Gopinatha K.R.[1], Gnaneshwari P[2], Dhananjaya M[3], Mallika K.S.[4]

[1]Department of Mathematics, Global Academy of Technology, Bangalore-560098, India.
E-mail: gopinathakr@gat.ac.in
[2]Department of Mathematics, Bangalore Institute of Technology, Bangalore-560004, India.
E-mail: gnaneshwarip@bit-bangalore.edu.in
[3]Department of Mathematics, Bangalore Institute of Technology, Bangalore-560004, India.
E-mail: dr.mdhananjaya@bit-bangalore.edu.in
[4]Department of Mathematics, Global Academy of Technology, Bangalore-560098, India.
E-mail: mallikaks@gat.ac.in

Corresponding author: Gopinatha K.R.
Department of Mathematics, Global Academy of Technology.
E-mail: gopinathakr@gat.ac.in

Received: 10/05/2026 **Revised**: 05/06/2026 **Accepted**: 02/07/2026

Abstract

The analytical study of viscous, incompressible, conducting fluid flow in multiple regions past and through an impermeable cylinder embedded in a sparsely packed porous medium in presence of transverse magnetic field is presented. Modified Brinkman equation and Stokes equation are used as governing equations. Here we have computed Tangential velocity component, Normal velocity component, streamlines and drag coefficient. The effect of dimensionless parameters on the fluid flow have been analyzed and presented graphically.

Key words: Modified Brinkman equation, Porous Parameter, Hartmann Number, Modified Bessel's equations, Magnetic permeability, Drag coefficient

INTRODUCTION

Fluid flow through or around permeable media is a fundamental phenomenon in numerous engineering and scientific applications, including geothermal energy systems, bioremediation processes, construction engineering, and many more. In particular, the roles of energy conversion and conservation have intensified the use of porous materials in advanced technologies such as fuel cells, thermal insulation systems, and electrochemical batteries.

One of the most critical branches of fluid mechanics in this context is magnetohydrodynamics (MHD), which studies the behaviour of electrically conducting fluids under the influence of magnetic fields. While the impact of MHD is minimal in terrestrial environments such as oceans or the atmosphere due to water's weak conductivity, its influence become profound in astrophysical and industrial contexts. Notable applications include solar wind modelling, dynamo theory, magnetic drug targeting, and magnetic resonance imaging (MRI) technology.

In industrial applications, MHD effects are often harnessed to control fluid flow around solid structures, particularly in the design of magnetically driven pumps, MHD generators, polymer processing, petroleum extraction, and heat exchanger technology. Among classical problems, Hartmann flow representing the flow of a conducting fluid between two parallel plates under a transverse magnetic field is of foundational significance and widely used as a benchmark for MHD studies.

In this study, we consider the steady, incompressible, viscous, and electrically conducting flow of fluid over a rigid cylinder of unit radius, which is enclosed first by a fluid region and then by a surrounding permeable medium, all embedded within an unbounded fluid domain. The system is subjected to a uniform transverse magnetic field, perpendicular to the direction of flow. The magnetic Reynolds number is assumed to be small, which justifies neglecting the induced magnetic field in comparison to the applied magnetic field an assumption commonly valid for most industrial fluids with low conductivity.

Power System Protection and Control
ISSN:1674-3415

An exact analytical solution is derived using similarity transformation techniques. The governing flow equations are solved individually in the fluid and porous regions using Stokes and Brinkman models, respectively. The boundary conditions include:

- No-penetration (impenetrability) at the rigid cylinder surface,
- Continuity of velocity and stress at the interface between fluid and porous regions,
- Asymptotic matching to a uniform free-stream velocity as r→∞.

This investigation contributes to the understanding of how porosity and magnetic field strength affect flow structure and resistance, which has practical implications in designing and optimizing fluid systems influenced by both magnetic and porous effects.

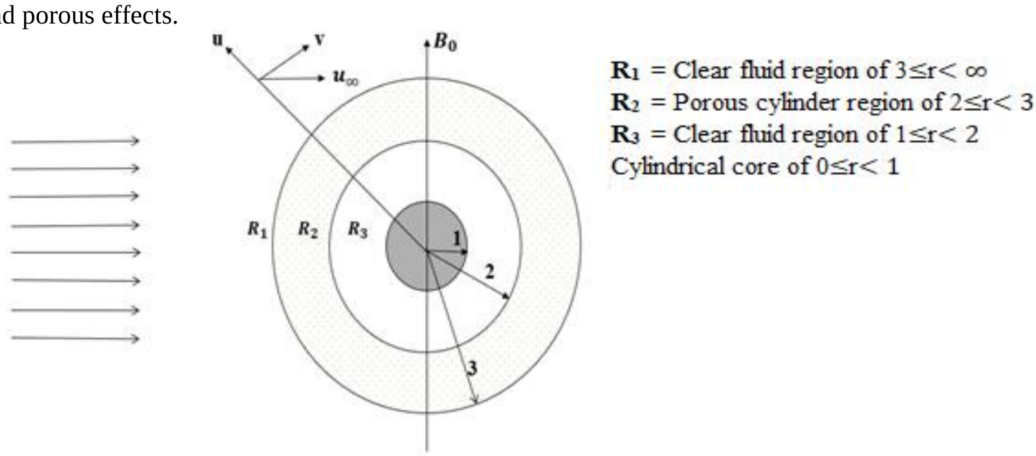

Physical Configuration

MATHEMATICAL MODELING

We consider the steady, two-dimensional, incompressible, viscous, and electrically conducting fluid flow past a fixed rigid cylinder of radius r=1, surrounded successively by a clear fluid region extending up to radius r=2, and a porous cylindrical shell extending further up to radius r=3. The entire domain is assumed to be immersed in an infinitely extended fluid region (r<∞), and the flow is subjected to a uniform transverse magnetic field perpendicular to the direction of flow.

In many industrial and engineering applications, the working fluids typically possess low electrical conductivity and small magnetic Reynolds numbers. Hence, the induced magnetic field is negligible in comparison to the externally applied magnetic field. Based on this assumption, the magnetohydrodynamic (MHD) approximation simplifies, and only the applied magnetic field is considered in the analysis.

The flow is also assumed to be axisymmetric, resulting in a simplification of the governing equations. The fluid motion occurs in three concentric regions:

- Region R1: Clear fluid region (1<r<2)
- Region R2: Porous medium (2<r<3)
- Region R3: Outer clear fluid region (3<r<∞)

Continuity equation $\nabla \cdot \overrightarrow{q_1} = 0$ (1)

Modified Stokes equation $\nabla p_1 = \mu \nabla^2 \overrightarrow{q_1} + \mu_h^2 \sigma_e \left(\overrightarrow{q_1} \times \vec{H}\right) \times \vec{H},$ (2)

In porous region (region R_2) the flow is characterized by the equations which are:

Continuity equation $\nabla \cdot \overrightarrow{q_2} = 0\,,$ (3)

Modified Brinkman equation

$$\nabla p_2 = \bar{\mu} \nabla^2 \overrightarrow{q_2} - \frac{\mu}{K} \overrightarrow{q_2} + \mu_h^2\, \sigma_e \left(\overrightarrow{q_2} \times \vec{H}\right) \times \vec{H}, \qquad (4)$$

Also, the flow in clear fluid section (region R_3) is represented by the equations

$$\nabla \cdot \overrightarrow{q_3} = 0, \qquad (5)$$

$$p_3 = \bar{\mu} \nabla^2 \overrightarrow{q_3} + \mu_h^2 \sigma_e \left(\overrightarrow{q_3} \times \vec{H}\right) \times \vec{H}, \qquad (6)$$

In addition, the hypothesis made here is, $\bar{\mu} = \mu$.

Power System Protection and Control
ISSN:1674-3415

We considered the cylindrical polar co-ordinates (r,θ,ϕ) with the origin as a center of the cylinder. All quantities are independent of ϕ since the flow is axially symmetric.
We introduce the following non-dimensional parameters:

$$r^*=\frac{r}{a},\ \overrightarrow{q_1^*}=\frac{\overrightarrow{q_1}}{u_\infty},\ \overrightarrow{q_2^*}=\frac{\overrightarrow{q_2}}{u_\infty},\ \overrightarrow{q_3^*}=\frac{\overrightarrow{q_3}}{u_\infty},p_1^*=\frac{a_1p_1}{\mu u_\infty},$$

$$p_2^*=\frac{a_1p_2}{\mu u_\infty},\ p_3^*=\frac{a_1p_3}{\mu u_\infty},\overrightarrow{H^*}=\frac{\overrightarrow{H}}{H_0} \qquad (7)$$

In the view of equation of continuity, one can define a stream function $\psi_j(r,\theta)$ (where $j=1,2,3$ for fluid, permeable and fluid regions respectively) such that

$$u_j=\frac{1}{r}\frac{\partial\psi_j}{\partial\theta};\quad v_j=-\frac{\partial\psi_j}{\partial r}, \qquad (8)$$

Removing the pressure term from the equations (2), (4) and (6) by cross multiplication method, an equation for ψ_j which is linear partial differential equation of 4th order can be obtained in the form

$$E^4\psi_j-{Q_j}^2E^2\psi_j=0, \qquad (9)$$

where $Q_j^2=\begin{cases}m^2, & j=1\\ s^2, & j=2\\ m^2, & j=3\end{cases}$ for fluid, permeable and fluid sections respectively.

The impenetrability conditions at the surface of the rigid cylinder is:

$$u_3(1,\theta)=0,\quad 0\le\theta\le 2\pi, \qquad (10)$$

$$v_3(1,\theta)=0,\quad 0\le\theta\le 2\pi. \qquad (11)$$

Matching interface conditions at the boundary of region R1 and region R2,

$$u_2(3,\theta)=u_1(3,\theta),\ 0\le\theta\le 2\pi, \qquad (12)$$

$$v_2(3,\theta)=v_1(3,\theta),\ 0\le\theta\le 2\pi, \qquad (13)$$

$$\tau_{r\theta(2)}(3,\theta)=\tau_{r\theta(1)}(3,\theta),\ 0\le\theta\le 2\pi, \qquad (14)$$

$$\tau_{rr(2)}(3,\theta)=\tau_{rr(1)}(3,\theta),\ 0\le\theta\le 2\pi, \qquad (15)$$

Also, at the boundary of region R2 and region R3,

$$u_3(2,\theta)=u_2(2,\theta),\ 0\le\theta\le 2\pi, \qquad (16)$$

$$v_3(2,\theta)=v_2(2,\theta),\ 0\le\theta\le 2\pi, \qquad (17)$$

$$\tau_{r\theta(3)}(2,\theta)=\tau_{r\theta(2)}(2,\theta),\ 0\le\theta\le 2\pi, \qquad (18)$$

$$\tau_{rr(3)}(2,\theta)=\tau_{rr(2)}(2,\theta),\ 0\le\theta\le 2\pi, \qquad (19)$$

Where

$$\tau_{r\theta(1)}=\frac{1}{r}\frac{\partial u_1}{\partial\theta}+\frac{\partial v_1}{\partial r}-\frac{v_1}{r},\quad \text{is the tangential stress component} \qquad (20)$$

$$\tau_{rr(1)}=-p_1+2\frac{\partial u_1}{\partial r}\quad \text{is the normal stress component} \qquad (21)$$

Further, $\tau_{r\theta(2)},\tau_{rr(2)}$ in region R2 and $\tau_{r\theta(3)},\tau_{rr(3)}$ in region R3 are also defined likewise as equation (20) and equation (21).

Since $\overline{\mu}=\mu$, we have

$$p_2(3,\theta)=p_1(3,\theta),\ 0\le\theta\le 2\pi, \qquad (22)$$

$$p_3(2,\theta)=p_2(2,\theta),\ 0\le\theta\le 2\pi. \qquad (23)$$

Further, the stream function for constant flow away from the boundary is:

$$\psi_1(r,\theta)=\left(r-\frac{1}{r}\right)\sin\theta,\quad 3\le r<\infty. \qquad (24)$$

From the equations (1) and (2), velocity components in region R1:

$$u_1\sim\cos\theta,\quad v_1\sim-\sin\theta \text{ as } r\to\infty. \qquad (25)$$

Therefore, the equation (2) becomes,

$$\psi_1(r,\theta)\sim r\sin\theta,\ \text{as } r\to\infty. \qquad (26)$$

SYSTEM OF SOLUTION

An equation (4) suggests the similarity solution to the equation (9) as:

$$\psi_j(r,\theta)=f_j(r)\sin\theta, \qquad (27)$$

where $j=1,2,3$ for fluid, permeable and fluid regions.

Solving equation (9) using equation (27), we obtain ordinary differential equation of 4th order as,

$$f_j^{iv}+\frac{2}{r}f_j'''-\frac{3}{r^2}f_j''+\frac{3}{r^3}f_j'-\frac{3}{r^4}f_i-{J_j}^2\left(f_j''+\frac{1}{r}f_j'-\frac{1}{r^2}f_j\right)=0, \qquad (28)$$

DOI: 10.46121/pspc.54.3.20

where $Q_j^2 = \begin{cases} m^2\,, & j=1 \\ s^2\,, & j=2 \\ m^2 & j=3 \end{cases}$ for fluid, permeable and fluid regions respectively.

The corresponding no-slip and interface boundary conditions in terms of $f_j(r)$, from the equations (12) to (21) are given as in the equations
No-slip condition at the surface of the rigid sphere is expressed by:

$$f_3(1) = 0, \tag{29}$$
$$f_3{}'(1) = 0, \tag{30}$$

and at the interface of region R_1 and region R_2, the boundary conditions are,

$$f_2(3) = f_1(3), \tag{31}$$
$$f_2{}'(3) = f_1{}'(3), \tag{32}$$
$$f_2{}''(3) = f_1{}''(3), \tag{33}$$
$$f_2{}'''(3) - \sigma^2 f_2{}'(3) = f_1{}'''(3). \tag{34}$$

also at the interface of region R_2 and region R_3, ,

$$f_3(2) = f_2(2), \tag{35}$$
$$f_3{}'(2) = f_2{}'(2), \tag{36}$$
$$f_3{}''(2) = f_2{}''(2), \tag{37}$$
$$f_2{}'''(2) - \sigma^2 f_2{}'(2) = f_3{}'''(2). \tag{38}$$

The uniform speed far from the boundary, the equation (26) becomes

$$f_1(r) \sim r \quad \text{as} \quad r \to \infty. \tag{39}$$

Take the substitution, $p_j(r) = f_j''(r) + \frac{1}{r} f_j'(r) - \frac{1}{r^2} f_j(r)$ (40)
to reduce ordinary differential equation of 4th order into 2nd order. Here suffix j takes the values from 1 to 3 which represents the solution respectively in fluid, permeable and fluid regions.
Using the equation (40) in the equation (28), we get

$$p_j''(r) + \frac{1}{r} p_j'(r) - \left[J_j^2 + \frac{1}{r^2}\right] p_j(r) = 0 \tag{41}$$

where $Q_j^2 = \begin{cases} m^2\,, & j=1 \\ s^2\,, & j=2 \\ m^2, & j=3 \end{cases}$

Equation (41) represents modified Bessel's differential equation of order one, whose general solution is given by:

$$p_j(r) = C_j K\left(Q_j r\right) + D_j I\left(Q_j r\right) \tag{42}$$

where C_j and D_j are arbitrary constants. From the equations (40) and (42), we get

$$f_j''(r) + \frac{1}{r} f_j'(r) - \frac{1}{r^2} f_j(r) = C_j K\left(Q_j r\right) + D_j I\left(Q_j r\right) \tag{43}$$

which is ordinary differential equation of 2nd order involving the variable coefficients which can be solved by variation of parameters method and gained the general solution as

$$f_j(r) = A_j r + \frac{B_j}{r} + C_j K\left(Q_j r\right) + D_j I\left(Q_j r\right) \tag{44}$$

Therefore, the solutions of equation (44) for fluid, porous and fluid region respectively are given by,

$$f_1(r) = A_1 r + \frac{B_1}{r} + C_1 K(mr) + D_1 I(mr), 3 \le r < \infty \tag{45}$$
$$f_2(r) = A_2 r + \frac{B_2}{r} + C_2 K(sr) + D_2 I(sr),\ 2 \le r < 3, \tag{46}$$
$$f_3(r) = A_3 r + \frac{B_3}{r} + C_3 K(mr) + D_3 I(mr), 1 \le r < 2 \tag{47}$$

As $r \to \infty, I(Mr) \to \infty$ in region R_1. Hence $D_1 = 0$ and further from the equation (39) we get $A_1 = 1$, Therefore Eq. (45) reduces to:

$$f_1(r) = r + \frac{B_1}{r} + C_1 K(mr), 3 \le r < \infty, \tag{48}$$

Thus, the stream function in fluid, permeable and fluid regions are given by,

$$\psi_1(r,\theta) = \left(r + \frac{B_1}{r} + C_1 K(mr)\right) \sin\theta, \tag{49}$$

DOI: 10.46121/pspc.54.3.20

$$\psi_2(r,\theta) = \left(A_2 r + \frac{B_2}{r} + C_2 K(sr) + D_2 I(sr)\right)\sin\theta\,, \qquad (50)$$

$$\psi_3(r,\theta) = \left(A_3 r + \frac{B_3}{r} + C_3 K(mr) + D_3 I(mr)\right)\sin\theta\,, \qquad (51)$$

where $B_1, C_1, A_2, B_2, C_2, D_2, A_3, B_3, C_3$ and D_3 are the arbitrary constants which are found with the help of boundary conditions mentioned from the equations (29) to (38).
The shearing stress at some point on the surface of the cylinder is given by

$$\tau_{r\theta} = \bar{\mu}\left(r\frac{\partial}{\partial r}\left(\frac{v}{r}\right) + \frac{1}{r}\frac{\partial u}{\partial\theta}\right) \qquad (52)$$

On non–dimensionalising, equation (52) reduces to

$$\frac{\tau_{r\theta}}{\frac{\bar{\mu}U_\infty}{a}} = -\left(\frac{1}{r}\frac{\partial u}{\partial\theta} + r\frac{\partial}{\partial r}\left(\frac{v}{r}\right)\right) \qquad (53)$$

$$\tau_{r\theta_i} = -\frac{\bar{\mu}U_\infty}{c}\left(3\frac{B_1}{r^3} - \frac{1}{r} + C_1\left(-\frac{K_1'(mr)m}{r} + K_1''(mr)m^2\right)\right)\sin\theta \qquad (54)$$

$$\tau_{r\theta_2} = -\frac{\bar{\mu}U_\infty}{c}\left(\begin{matrix}\frac{4B_2}{r^3}4 - 2A_2 + C_2\left[s^2\left(I_1''(sr) - \frac{K_1'(Sr)S}{r}\right)\right] + \\ D_2\left[\left(s^2 I_1''(sr) - \frac{K_1'(Sr)S}{r}\right)\right]\end{matrix}\right)\sin\theta. \qquad (55)$$

$$\tau_{r\theta_3} = -\frac{\bar{\mu}U_\infty}{c}\left(\begin{matrix}\frac{4B_3}{r^3}4 - 2A_3 + C_3\left[m^2\left(I_1''(mr) - \frac{K_1'(mr)m}{r}\right)\right] + \\ D_2\left[\left(m^2 I_1''(mr) - \frac{K_1'(mr)m}{r}\right)\right]\end{matrix}\right)\sin\theta. \qquad (56)$$

The equations (54)-(56) represent shearing stress equation for fluid, porous and fluid region respectively.

SOLVE FOR THE DRAG FORCE

The drag force F_t for an impermeable cylinder of radius 'a' embedded in a porous medium can be calculated by integrating the stresses over the impermeable cylinder as

$$F_t = \int_0^{2\pi}\int_0^{\pi}\{(\tau_{r\theta})_{r=a}\}\,R^2\sin\theta\,d\varphi\,d\theta \qquad (57)$$

Substituting equation (54) -(56) in equation (57), we get:

$$F_{t1} = 4\pi\bar{\mu}U_\infty a G_1 \quad F_{t2} = -4\pi\bar{\mu}U_\infty a G_2 \quad F_{t3} = -4\pi\bar{\mu}U_\infty a G_3 \qquad (58)$$

Further, the drag coefficient is given by:

$$C_D = \frac{F_{ti}}{-\frac{1}{2}\rho U_\infty^2 a^2\pi} \qquad (59)$$

Substituting equation (58) in equation (59), we get:

Drag co-efficient in fluid region

$$C_{D_1} = \frac{16G_1}{R_e} \qquad (60)$$

Drag co-efficient in porous region

$$C_{D_2} = \frac{16}{R_e}G_2 \qquad (61)$$

Drag co-efficient in fluid region

$$C_{D_2} = \frac{16}{R_e}G_3 \qquad (62)$$

where $R_e = \dfrac{2\rho U_\infty a}{\bar{\mu}}$ is Reynolds number.

$$G_1 = -\frac{\bar{\mu}U_\infty}{c}\left(3\frac{B_1}{r^3} - \frac{1}{r} + C_1\left(-\frac{K_1'(mr)m}{r} + K_1''(mr)m^2\right)\right) \qquad (63)$$

$$G_2 = -\frac{\bar{\mu}U_\infty}{c}\left(\begin{matrix}\frac{4B_2}{r^3}4 - 2A_2 + C_2\left[s^2\left(I_1''(sr) - \frac{K_1'(Sr)S}{r}\right)\right] + \\ D_2\left[\left(s^2 I_1''(sr) - \frac{K_1'(Sr)S}{r}\right)\right]\end{matrix}\right) \qquad (64)$$

DOI: 10.46121/pspc.54.3.20

$$G_3 = -\frac{\bar{\mu} U_\infty}{c}\left(\begin{array}{c}\frac{4B_3}{r^3}4 - 2A_3 + C_3\left[m^2\left(I_1''(mr) - \frac{K_1'(mr)m}{r}\right)\right] + \\ D_2\left[\left(m^2 I_1''(mr) - \frac{K_1'(mr)m}{r}\right)\right]\end{array}\right) \quad (65)$$

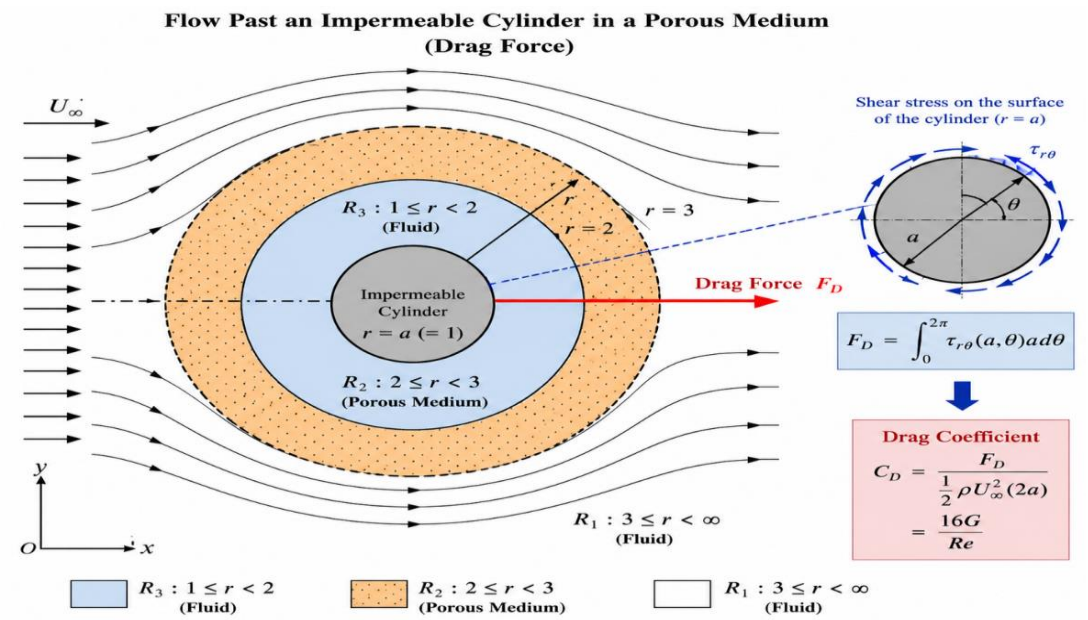

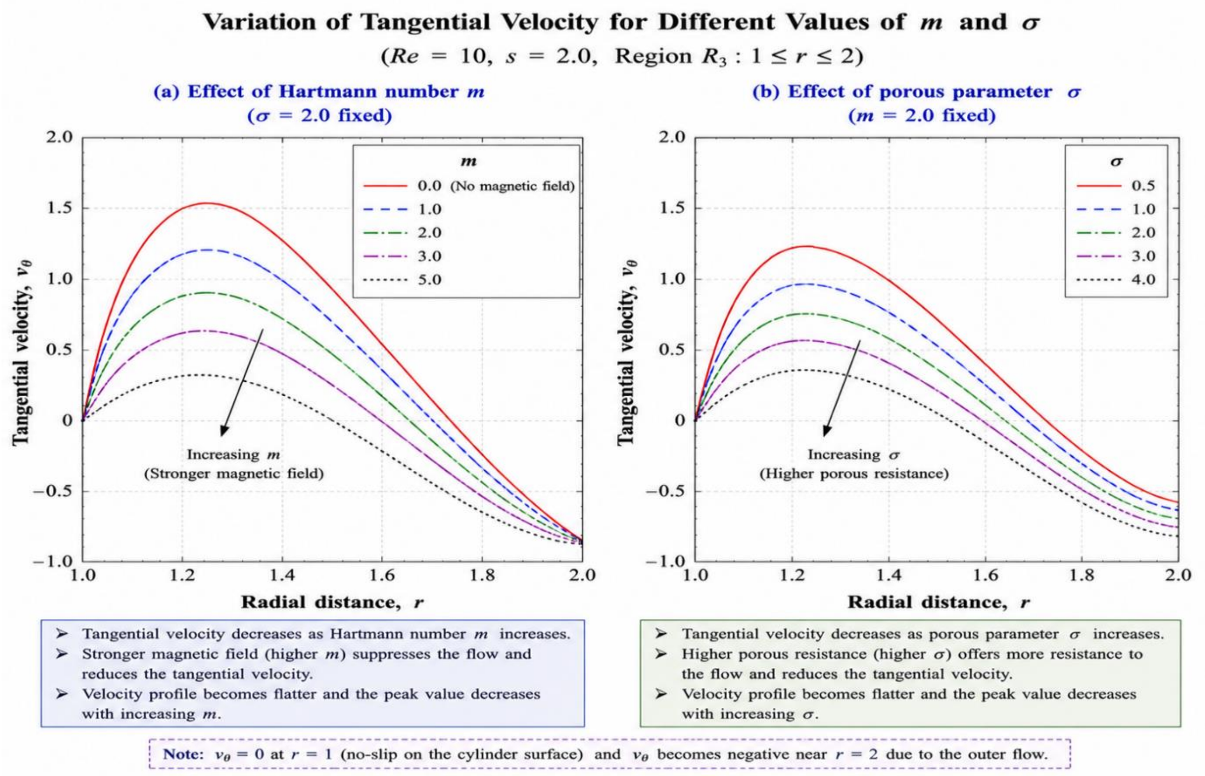

DOI: 10.46121/pspc.54.3.20

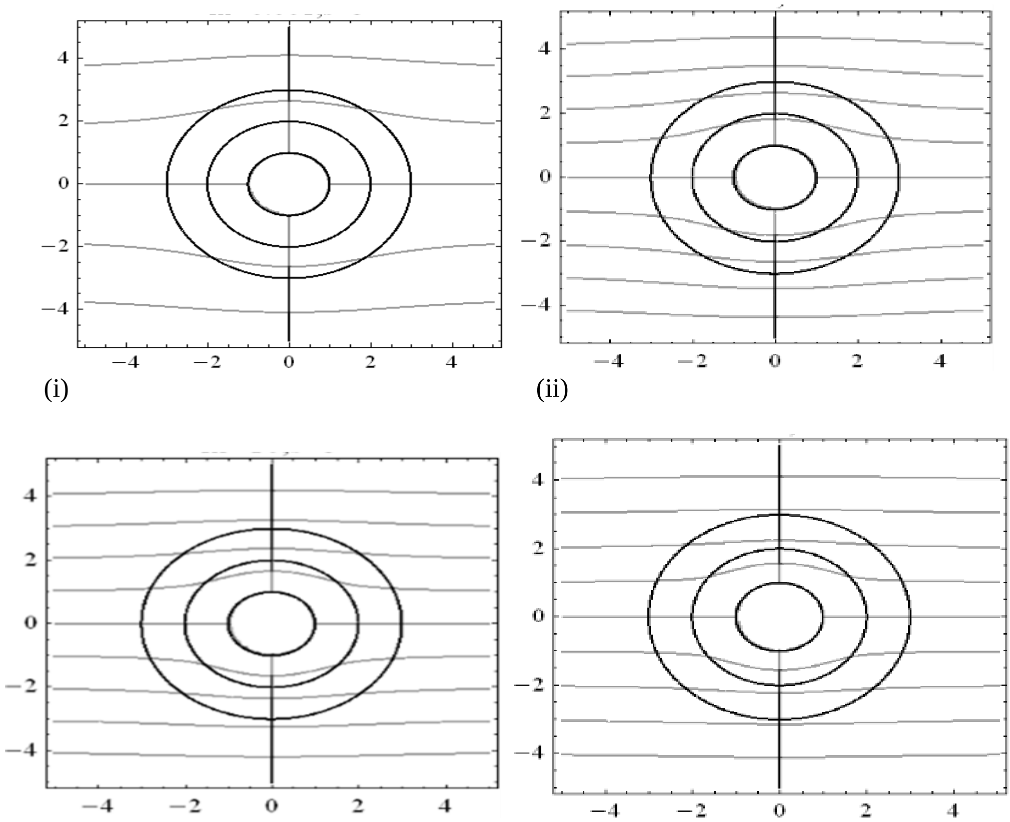

(i) (ii) (iii) (iv)

Figure.1 Streamlines for fixed $\sigma = 5$ and varying m

(i) m = 0.001 (ii) m = 6 (iii) m = 10 (iv) m = 20.

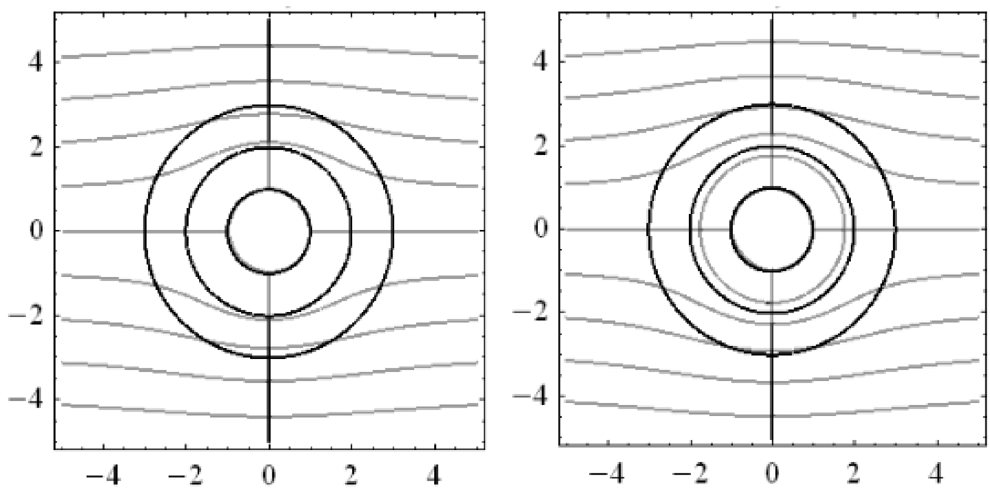

(i) (ii)

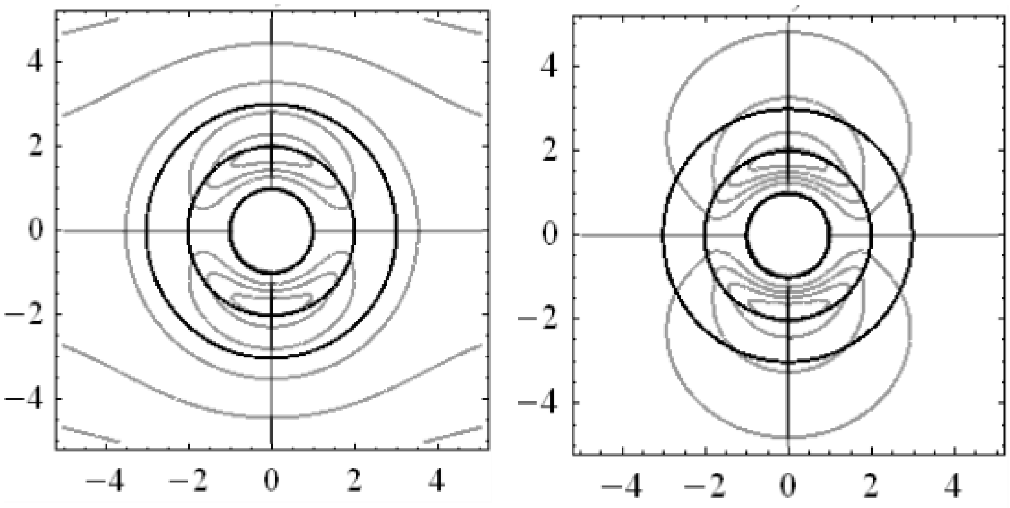

(iii) (iv)

Figure. 2 Streamlines for fixed $m = 0.01$ and varying values of σ

(i) σ = 5 (ii) σ = 5.5 (iii) σ = 6 (iv) σ = 6.4

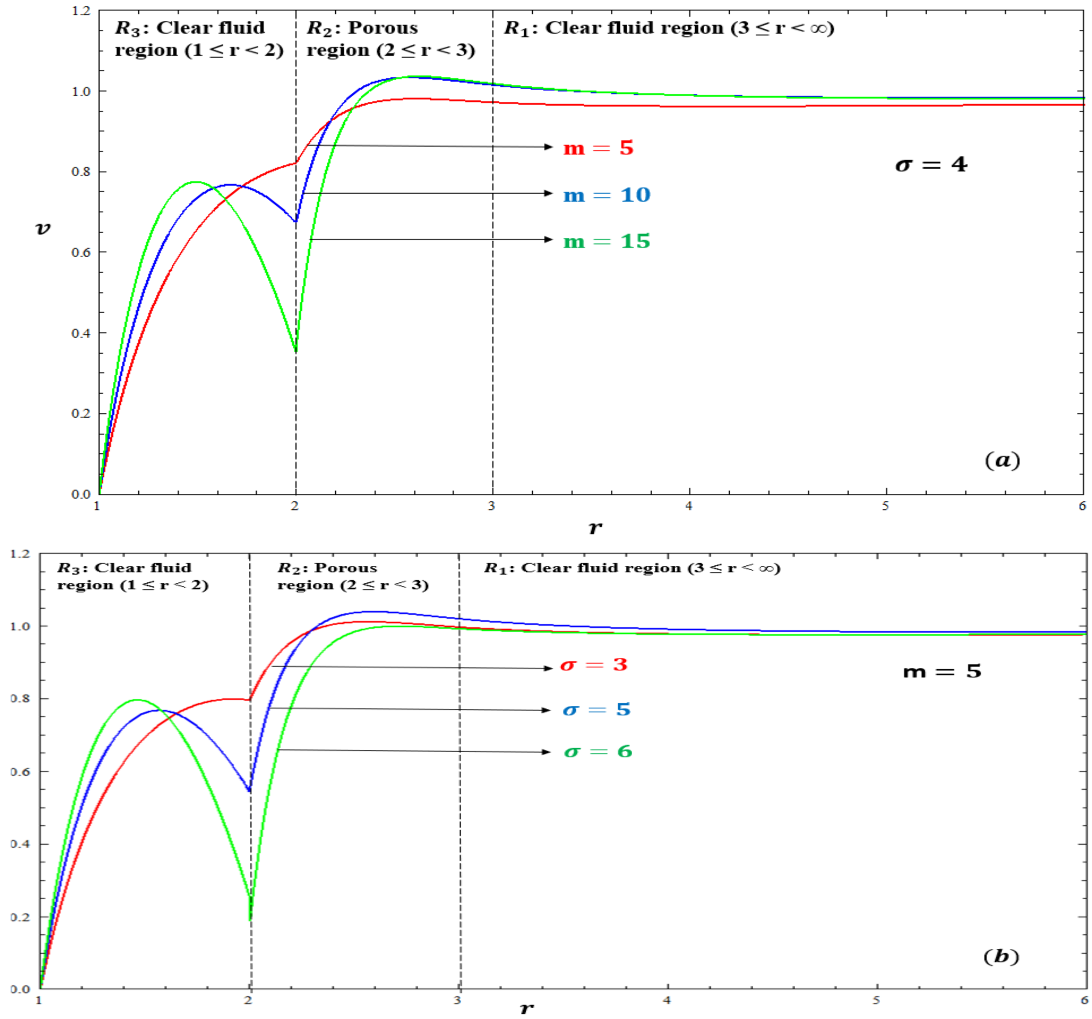

Figure. 3 Variation of tangential velocity for different values of m and σ

DOI: 10.46121/pspc.54.3.20

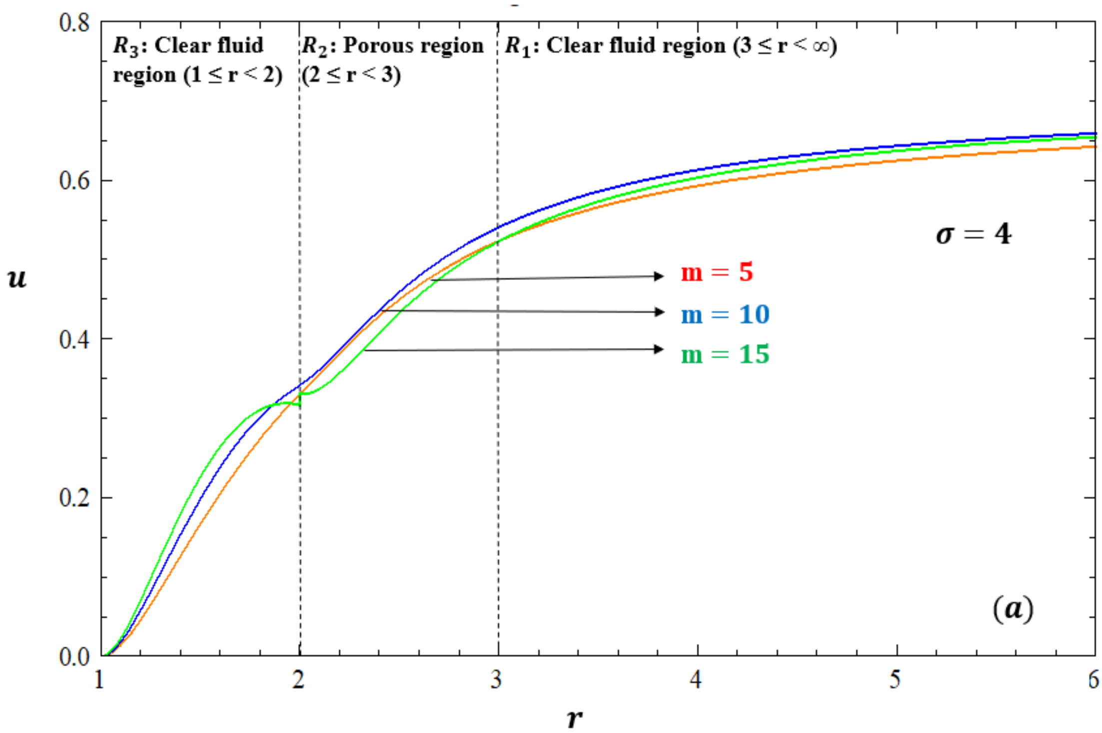

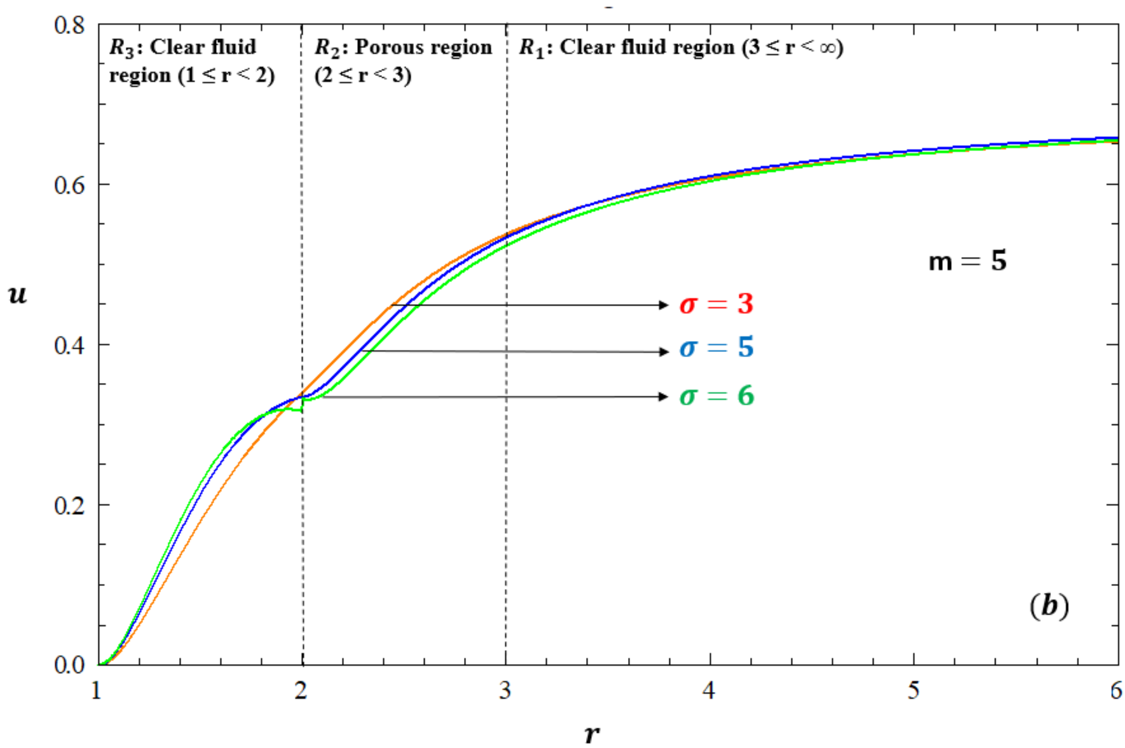

Figure. 4 Variation of normal velocity for different values of m and σ

Power System Protection and Control
ISSN:1674-3415

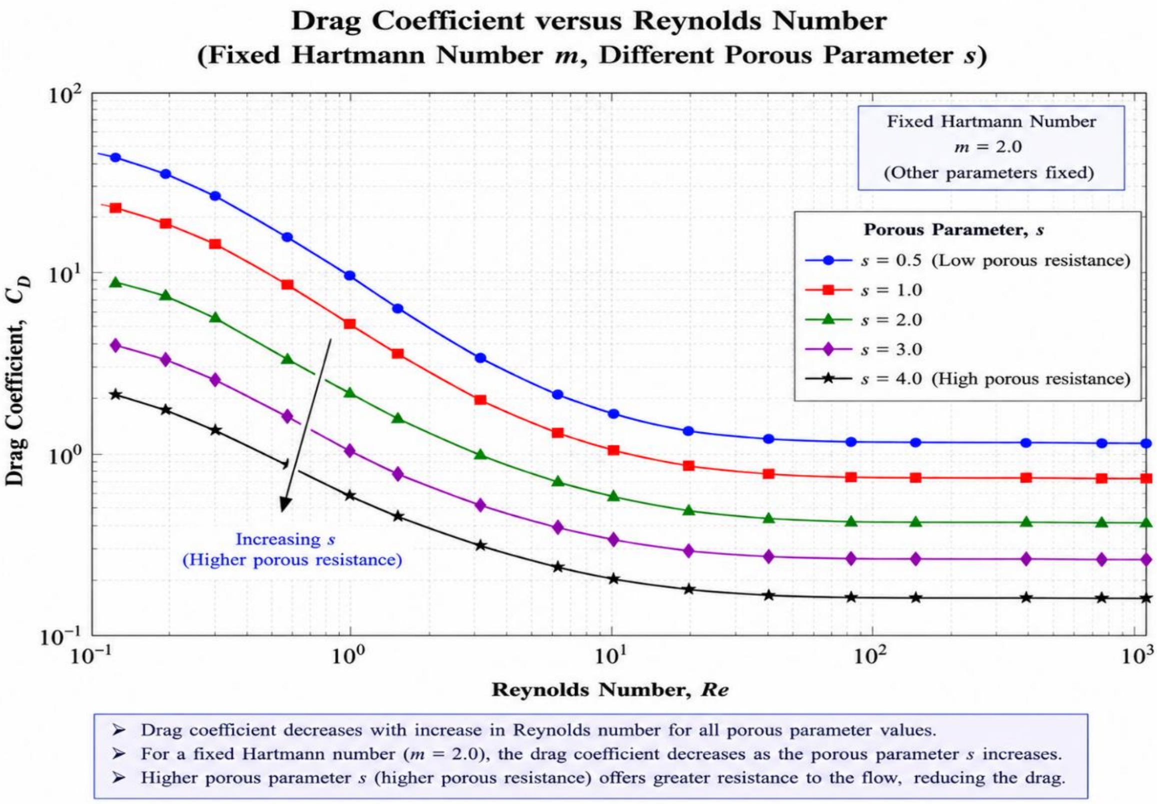

Figure.5: Drag co-efficient for fixed Hartmann number m and different values of porous parameter σ .

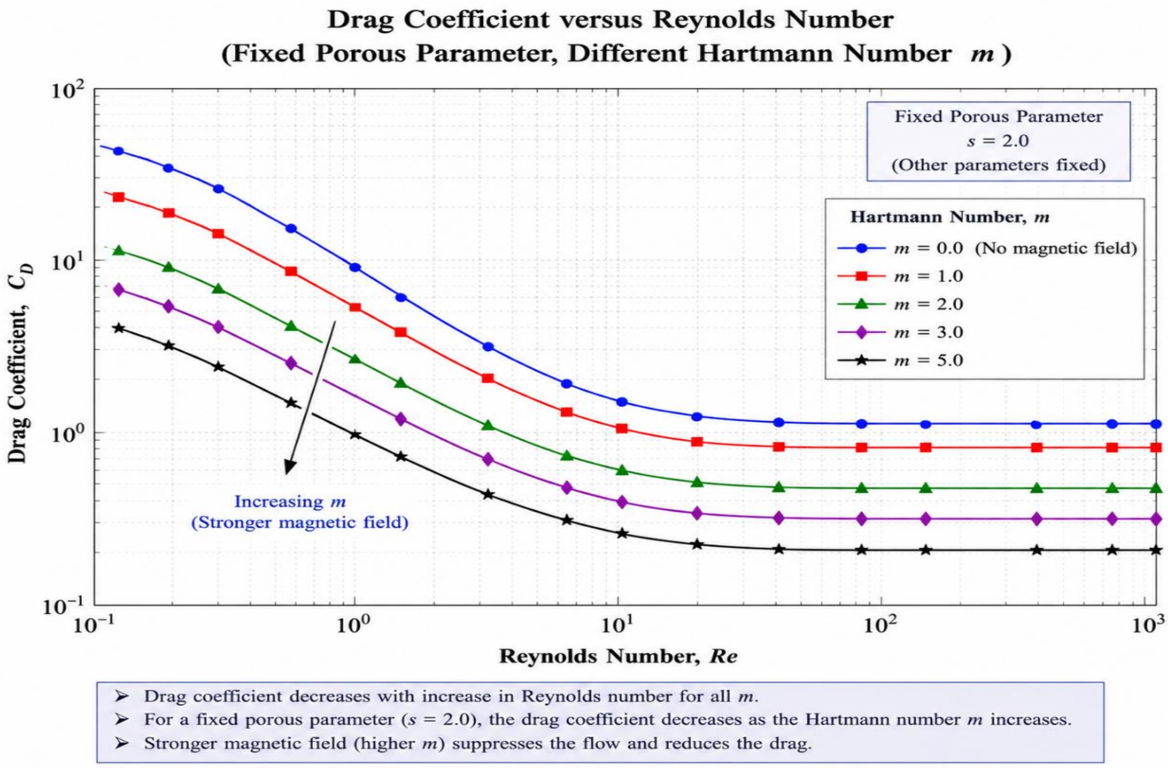

Figure.6: Drag co-efficient for fixed porous parameter σ and different values of Hartmann number m

Power System Protection and Control
ISSN:1674-3415

RESULTS AND DISCUSSIONS

This section presents a comprehensive analysis of the flow behavior, streamline patterns, velocity components, and drag coefficient for an incompressible, viscous, and electrically conducting fluid flowing around a rigid cylinder, influenced by an external magnetic field and a surrounding porous medium. The modified Stokes and Brinkman equations are employed to model the flow in the clear and porous regions, respectively. The exact solutions are obtained using similarity transformations and expressed in terms of modified Bessel functions. The influence of key non-dimensional parameters such as the Hartmann number 'm' and the porosity parameter σ is analyzed.

Streamline Performance under Magnetic and Porosity Effects
The effect of magnetic field strength and porous permeability on the fluid flow is studied through streamline plots. When the porosity parameter is increased to σ=5 and the magnetic field is negligible (m=0.001), the resistance offered by the porous medium significantly reduces fluid penetration, resulting in weaker streamline intensity in the porous region (Figure 1(i)). With increasing magnetic field, fluid re-entry into the porous region is enhanced, and streamlines once again begin to encircle the solid cylinder (Figures 1(ii)–(iv)).

Conversely, for fixed low magnetic field m=0.01, increasing the porosity parameter from σ=5 to σ=6.4 reduces the permeability of the porous region. As a result, fluid penetration decreases and flow recirculation or circulatory motion becomes prominent within the porous region, as shown in Figures 2(i)–(iv).

Tangential and Normal Velocity Distribution
Tangential velocity profiles are examined along the line θ=π/2 across the three regions: clear fluid (inner and outer) and porous medium. For fixed σ =4, increasing the magnetic field suppresses velocity in the porous region due to the Lorentz force, while velocity recovers in the outer clear fluid region. The velocity profile assumes a parabolic shape, with the maximum occurring in the mid-porous region and minima at the solid core (no-slip condition) and fluid–porous interface (matching condition), as shown in Figure 3(i).

For a fixed magnetic field m=5, increasing σ leads to reduced velocity due to diminished permeability. This confirms that the porosity parameter plays a significant role in moderating the velocity field (Figure 3(ii)).

Normal velocity variations are analyzed along θ=π/4 for both increasing Hartmann number and porous parameter. With higher magnetic fields, the normal velocity decreases within the porous zone, slightly increases near the interface due to continuity constraints, and again decreases in the outer region. A similar pattern is observed for increasing σ, where the fluid's ability to penetrate and circulate within the porous region is reduced (Figures 4(i) and 4(ii)).

Drag Coefficient for Fixed Hartmann Number m and Different Values of Porous Parameter σ, and vice versa
The figure 5 illustrates the variation of the drag coefficient C_D with Reynolds number Re for a fixed Hartmann number m and different values of the porous parameter σ.

It is observed that the drag coefficient decreases monotonically with increasing Reynolds number for all values of the porous parameter σ. At low Reynolds numbers, viscous effects dominate the flow, resulting in higher drag coefficients. As the Reynolds number increases, inertial effects become more significant, leading to a reduction in drag.

The influence of the porous parameter σ is also clear from the figure 5. For a fixed Reynolds number, the drag coefficient decreases as the porous parameter increases. The curve corresponding to the smallest porous parameter exhibits the highest drag coefficient, whereas the curve corresponding to the largest porous parameter gives the lowest drag coefficient.

Physically, a larger porous parameter corresponds to higher permeability resistance within the porous layer. The porous medium absorbs a greater portion of the fluid momentum and suppresses fluid motion near the cylinder surface. Consequently, the velocity gradients and wall shear stresses are reduced, leading to a lower drag force acting on the cylinder.

Furthermore, the separation between the curves is more pronounced at lower Reynolds numbers and gradually diminishes at higher Reynolds numbers. This indicates that the influence of the porous parameter is strongest in the creeping-flow regime and becomes less significant as inertial effects dominate the flow field.

Therefore, the results demonstrate that increasing the porous parameter effectively reduces the drag coefficient of the cylinder, while increasing the Reynolds number further enhances this drag-reduction effect.

For a fixed magnetic field strength (m), increasing the porous parameter (σ) reduces the drag experienced by the impermeable cylinder embedded in the porous medium. This demonstrates the effectiveness of the porous layer in controlling and reducing hydrodynamic drag.

Conversely, the drag coefficient (C_D) decreases with increasing Hartmann number (m) for a fixed porosity parameter (σ). This reduction indicates lower fluid drag in the porous region due to the enhanced magnetic damping effect, as shown in Figure 6.

Main Observations

- C_D decreases with increasing Reynolds number Re.
- For fixed Hartmann number m, C_D decreases as a porous parameter increases.
- Maximum drag occurs for the smallest value of σ.
- Minimum drag occurs for the largest value of σ.
- The effect of σ is more significant at low Reynolds numbers.
- At high Reynolds numbers, all curves tend to approach nearly constant values.

REFERENCES

1. SAFFMAN P.G, “On the boundary condition at the surface of a porous medium”, ***Studies in Applied Mathematics,*** Volume.50, pp.93-101, **1971.**
2. BREAVERS G. S & JOSEPH D. D, “Boundary conditions at a naturally permeable wall”, ***J. Fluid Mech,*** Volume 30(1), pp.197-207, **1967.**
3. RAJA SEKHAR G.P & AMARANATH T, “Stokes flow past a porous sphere with an impermeable core”, ***Mechanics Research Communications,*** Volume 23(5), pp.449-460, **1996.**
4. RUDRAIAH N & CHANDRASHEKARA B.C, "Flow of conducting fluid between porous disks for large suction Reymolds number". ***J. Phys. SOC. Japan.,*** Vol. 27(4), 1041-1045 ,**1969**.
5. RUDRAIH N & CHANDRASEKHARA B.C, "MHD laminar flow between porous disks". ***Applied Sci. Res.,*** Vol.23, 42-52 ,**1970**.
6. NALINAKSHI.N, DINESH.P. A, SHIVAKUMARA.I. S CHANDRASHEKHAR.D. V, “Numerical solution for mixed convection heat transfer from a vertical heated plate embedded in a sparsely packed porous medium” ***Mapana Journal of Sciences.,*** Volume. 10, No. 2, pp. 37-52, **2011.**
7. DINESH P A, NALINAKSHI.N & CHANDRASHEKAR.D. V, “Soret and Dufour effects on mixed convection heat and mass transfer with variable fluid properties**”, *International Journal of Mathematical Archive.,*** Volume 4, No.11, pp.203-215, **2013.**
8. CHANDRASHEKHAR.D. V, DINESH.P. A & NALINAKSHI. N, “Shooting method to study mixed convection past a vertical heated plate with variable fluid properties and internal heat generation”, ***Mapana Journal of Sciences.,*** Volume 13, No.3, pp. 31-50, **2014**.
9. PADMAVATHI B.S., AMARANATH T., &PALANIAPPAN D “Stokes flow about a porous sphereical particle”, **Arch**. **Mechanics.,** Vol. 46[1-2], pp. 191-199**,**1994.
10. POP I., & INGHAM D.B., “Flow past a sphere embedded in a porous medium based on Brinkman model”, ***Int. Comm. Heat Mass Trans.,*** Vol. 23 [6], pp. 865-874,**1996**
11. SRINIVASCHARY D., & MURTHY J.V.R., “Flow past an axi-symmetric body embedded in a saturated porous medium”, ***C.R Mechanique.,*** Vol. 330, pp. 417-423,**2002.**
12. SATHY DEO & DUTTA D., “Stoke’s flow past a fluid prolate spheroid”, ***Indian J. Pure& Appl. Math.,***

DOI: 10.46121/pspc.54.3.20

vol. 95, no. 1, pp. 63–72**, 2003**.

13. DUANE R MIKULENCAK &JEFFREY F MORRIS, “Sationary shear flow around fixed and free bodies at finite Reynolds number”, ***J. Fluid Mech.,*** vol.100, pp.1-28, **2004.**
14. RUDRAIAH N & CHANDRASHEKARA B.C, "Flow past an impermeable sphere embedded in a porous medium with Brinkman model", ***Int J. Appl. Mech.Engng.,*** Vol. 10, 145-158 ,**2005.**
15. NALINAKSHI.N, DINESH.P. A & CHANDRASHEKHAR. D.V, “effects of variable fluid properties and MHD on mixed convection heat transfer from a vertical heated plate embedded in a sparsely packed porous medium”, ***IOSR Journal of Mathematics [IOSR-JM],*** e- ISSN: 2278-5728, ISSN: 2319-765X, Volume 7, Issue 1, pp. 20-31,**2013.**
16. BASANT K JHA, BABATUNDE AINE & AJIYA.A. T, “Role of suction / injection on MHD natural convection flow in a vertical microchannel”, ***International Jounal of Energy and Technology,*** Volume 7,**2015**.
17. P APARN, J.V RAMANA MURTHY & G. NAGARAJU, “Couple on a rotating permeable sphere in a couple stress fluid”, **Ain Ahams Engineering Journal,** Volume 9(4), pp. 665-673, **2018**
18. RAMALAKSHMI KRISHNAN & PANKAJ SHUKLA “creeping flow of couple stress fluid past a fluid sphere with a solid core”, **Journal of Applied Mathematics and Mechanics,** volume 101(11), **2021**
19. RAMALAKSHMI & PANKAJ SHUKLA, “Drag on a porous sphere embedded in micropolar fluid”, ***Int. J. of Applied mathematics*,** vol 109 No. 10, pp.181-189, **2016**.
20. JIZE SUI, PENG ZHAO, ZHENDONG CHENG & MASAO DOI, “A novel investigation of a micropolar fluid characterized by nonlinear Constitutive diffusion model in boundary layer flow and heat transfer”, ***Physics of fluids***, Vol 29, 023105, **2017**
21. SUDHIR PATEL, DINESH. P.A, SUMA.S. P & SRINIVAS.G, “Characteristic study of combined effect of MHD and coriolos force on free convection in a rectangular cavity with isotropic and anisotropic porous media”, ***Mapana Journal of Science.,*** Volume 18, No.3, pp.13-31, https://doi.org/10.12723/mjs.50.2, **2019**
22. NALINAKSHI.N, DINESH.P. A & CHANDRASHEKHAR. D.V, “Internal heat generation effect on mixed convection heat and mass transfer over a vertical heated plate with soret and dufour effects”, Sixth International Conference on Porous Media and its Applications in Science***, Engineering, and Industry, Eds, ECI Symposium Series.***, **2016.**
23. QIN YU & KALONI P. N., "Creeping flow past a porous spherical shell" **ZAMM,** Vol.73, 77-84 ,**1993**
24. PADMAVATHI B.S., & AMARANATH T., A solution for the problem of flow past a porous sphere". **ZAMP**, Vol.44, pp. 178-184, **1993**
25. N. RUDRIAH, MALLIKA K S, & N. SUJATHA.,**“**Electrohydrodynamic dispersion with interphase mass transfer in poorly conducting couple stress fluid bounded by porous layers”, Journal of Applied Fluid Mechanics (**JAFM**), Volume 9, number 1, pp. 71-81, January **2016**.
26. MALLIKA K S. & N. RUDRIAH., “Generalized dispersion of unsteady convective diffusion in couple stress poorly conducting fluid bounded by porous layer in the presence of an electric field”, World Journal of Engineering (**WJOE**), Volume 8, Number 4, pp. 335-346, **2011**.